G. GRITZNER[1],✉

M. KOPPE[1]

K. KELLNER[1]

J. PRZEWOZNIK[2]

J. CHMIST[2]

A. KOLODZIEJCZYK[2]

K. KROP[3]

Preparation and properties of La$_{0.67}$Pb$_{0.33}$(Mn$_{1-x}$Fe$_x$)O$_3$ compounds

[1] Institute for Chemical Technology of Inorganic Materials, Johannes Kepler University, 4040 Linz, Austria
[2] Department of Solid State Physics, AGH University of Science and Technology, 30-059 Krakow, Poland
[3] Department of Physics, Rzeszow University of Technology, 35-959 Rzeszow, Poland

ABSTRACT La$_{0.67}$Pb$_{0.33}$(Mn$_{1-x}$Fe$_x$)O$_3$ materials with $x = 0$, 0.01, 0.03, 0.06, 0.1, 0.15 have been prepared by a wet chemical malic acid gel method followed by heat treatment at 1000 °C in air or oxygen. X-ray diffraction showed that the compounds were phase pure. The crystal structure of the compounds were interpreted in the rhombohedral space group ($R\overline{3}c$). The temperature dependence of the resistance depended strongly on the Fe-content and showed metal–insulator transitions for all compounds. The Curie temperatures were determined from the dependence of the magnetization on the temperature and on the magnetic field. Both the Curie temperatures and saturation magnetic moments decreased linearly with increasing iron content. The metal–insulator transitions did not coincide with the relevant Curie temperatures. Reasons for this behavior are discussed.

PACS 72.80.Ga; 75.47.Lx; 75.60.Ej

1 Introduction

The rediscovery of the influence of the magnetic field on the resistance of lanthanum manganates in the early 1990's strongly enhanced research in this area [1]. Numerous papers on rare earth manganates of the general composition (L$_{1-x}$M$_x$)MnO$_3$, where L is La^{3+}, Sm^{3+}, Pr^{3+}, Nd^{3+} and M is Ca^{2+}, Sr^{2+}, Ba^{2+}, Cd^{2+} and Pb^{2+} have been published. Most of these studies are summarized in a review article [2].

Lead doped lanthanum manganate, the material of this investigation, is a room temperature ferromagnet with magnetoresistance behaviour. Pb-doped lanthanum manganates were first reported during a study of ionic ferromagnets of the general composition (La$_{1-x}$M$_x$)MnO$_3$, where M was a divalent cation, either Ca^{2+}, Sr^{2+}, Ba^{2+}, Cd^{2+} or Pb^{2+} [3]. Single crystals of the composition (La$_{1-x}$Pb$_x$)MnO$_3$ with x ranging from 0.26 to 0.43 were prepared and their structure was analyzed [4]. Magnetic properties and ordering of (La$_{0.5}$Pb$_{0.5}$)MnO$_3$ was published [5]. Pb-doped lanthanum manganates with partial substitution of Mn by transition metal cation such as Fe, Co or Ni were investigated [6, 7]. The structural and magnetic properties of (La$_{0.7}$Pb$_{0.3}$)(Mn$_{1-x}$Fe$_x$)O$_3$

x	La$_2$O$_3$ / g	PbO / g	Fe-citrate monohydrate / g	MnCO$_3$ / g
0	5.457	3.683	0	5.747
0.01	5.457	3.683	0.138	5.689
0.03	5.457	3.683	0.413	5.574
0.06	5.457	3.683	0.826	5.402
0.10	5.457	3.683	1.377	5.172
0.15	5.457	3.683	2.064	4.885

TABLE 1 Amounts of the starting materials for the preparation of La$_{0.67}$Pb$_{0.33}$(Mn$_{1-x}$Fe$_x$)O$_3$

with $x = 0.0$, 0.05, 0.1, 0.2 and 0.3 were reported [7]. Samples with x greater than 0.2 showed insulating behavior and are thus without interest as magnetoresistance material [7].

In this work we focus on structural, resistance and magnetic properties of La$_{0.67}$Pb$_{0.33}$(Mn$_{1-x}$Fe$_x$)O$_3$ materials with moderate doping level of $x = 0$, 0.01, 0.03, 0.06, 0.1, 0.15 where the linear decrease of ferromagnetic transition temperature and maximum of colossal magnetoresistance effect at the metal–insulator transition as a function of iron doping has been observed.

2 Experimental

2.1 Preparation and analysis

The precursor material was prepared via a malic acid gel technique. This technique allows mixing of the cations on a molecular level, thus facilitating the formation of phase pure material. The respective amounts of La$_2$O$_3$, PbO, MnCO$_3$ and iron citrate monohydrate (C$_6$H$_5$FeO$_7 \cdot$H$_2$O) used in a typical preparation are given in Table 1. The actual iron content in the monohydrate was derived from a thermogravimetric analysis. The powders were added to 150 ml of acetic acid and the suspension was heated to the boiling point under stirring for 30 minutes. The mixture was then diluted with 150 ml of distilled water and boiling was continued for another 30 minutes. 1.5 g of DL-malic acid was then introduced into the solution. The solvent was slowly evaporated until a gel was formed. The gel was dried at 125 °C and a pressure of 3 mbar for two hours. The dried gel was calcined at 800 °C. To avoid rapid decomposition of the gel a heating rate

✉ Fax: +43-70-2468-8905, E-mail: gerhard.gritzner@jku.at

of $1\,K\,min^{-1}$ was chosen up to 350 °C. The heating rate to 800 °C was $4\,K\,min^{-1}$. The powder was kept at 800 °C for 10 hours. The cooling rate was $5\,K\,min^{-1}$. The calcined material was ground in a micro-mill and then compacted into discs with a diameter of 10 mm with 10 kN. The specimens were sintered at 1000 °C. The heating rate to 700 °C was $5\,K\,min^{-1}$ and from 700 °C to 1000 °C $1\,K\,min^{-1}$. The samples were kept at 1000 °C for 10 hours. The cooling rate was $5\,K\,min^{-1}$.

The oxygen content was analyzed by an iodometric titration. 50 to 100 mg of the material was weighted with a precision of 0.1 mg into a titration flask. 10 ml of a freshly prepared aqueous solution of KI ($50\,g\,dm^{-3}$), 10 ml of concentrated hydrochloric acid and 80 ml of distilled, de-aerated water were added. The mixture was then heated to 50 °C until a clear solution was obtained. Using starch as an indicator, we titrated the iodine formed with a $0.05\,mol\,dm^{-3}$ solution of sodium thiosulfate. The oxygen stoichiometry was calculated according to:

$$x = s + \frac{Mw\,b\,f}{(16(a - b\,f))}$$

x: stoichiometric coefficient for oxygen, s: oxygen stoichiometry of the reduced form ($s = (1.2*0.67) + 0.33 + 1 = 2.335$), Mw: molecular weight of the reduced form $[g\,mol^{-1}]$ ($0.67LaO_{1.5} + 0.33CaO + xFeO + (1-x)MnO$), b: ml of $0.05\,mol\,dm^{-3}$ $Na_2S_2O_3$, f: stoichiometric coefficient of the $Na_2S_2O_3$ ($f = 0.0004$ for $0.05\,mol\,dm^{-3}$ $Na_2S_2O_3$), a: mass of the sample $[g]$.

2.2   Apparatus

X-ray diffraction spectra were measured on a Rigaku Geigerflex II D (40 kV, 20 mA) with Ni-filtered Cu K_α radiation. Rietveld analysis of the spectra was carried out with the PROGRAM FULLPROF (Version 3.5 - Dec97-LLB JRC) [8]. Scanning electron micrographs were acquired on a Jeol 6400 electron microscope (Japan). Energy dispersive X-ray fluorescence (EDX) was carried out with the help of a Röntec (Germany) system. The temperature dependence of the resistance was derived from the four-point technique. The temperature was measured with a Pt-100 thermometer. Specific resistances (resistivities) were obtained by the van der Pauw method.

Magnetic characterization of the samples were carried out with a standard vibrating sample magnetometer (VSM) in applied magnetic fields up to 1 T from 77 K up to room temperature. The dc magnetization was recorded during heating in applied dc fields of 50 Oe and 1000 Oe after zero-field cooling (ZFC) of the sample down to 77 K. Magnetization was measured for the powdered specimens.

3   Results and discussion

The thermogravimetric analysis of the precursor malic acid gel showed the rapid decomposition of the acetates and the organic material between 200 and 350 °C (Fig. 1). The weight loss at temperatures above 1100 °C is due to the disappearance of PbO, limiting the temperature for the preparation of the samples to 1000 °C.

X-ray diffraction studies on the calcined powders, the samples sintered at 1000 °C in air and in oxygen showed
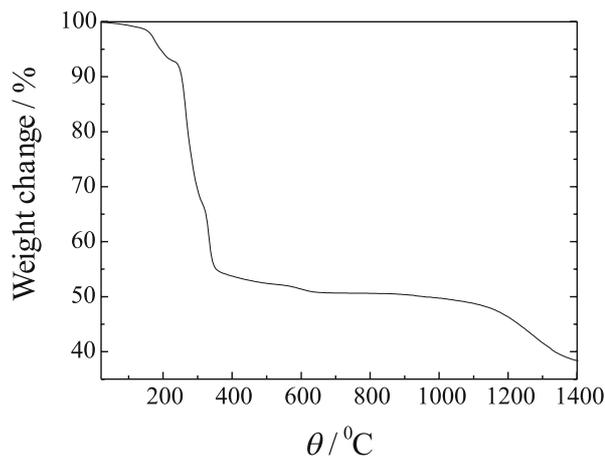
FIGURE 1   Thermogravimetric analysis of the precursor malic acid gel
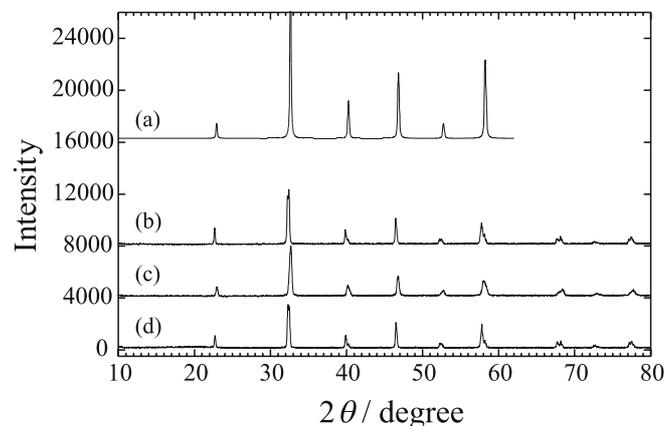
FIGURE 2   X-ray diffractograms of (a) LaMnO$_3$, (b) La$_{0.67}$Pb$_{0.33}$ (Mn$_{0.85}$Fe$_{0.15}$)O$_3$ sintered in oxygen (c) precursor powder for La$_{0.67}$Pb$_{0.33}$ (Mn$_{0.85}$Fe$_{0.15}$)O$_3$ calcined at 800 °C, and (d) La$_{0.67}$Pb$_{0.33}$(Mn$_{0.85}$Fe$_{0.15}$)O$_3$ sintered in air at 1000 °C
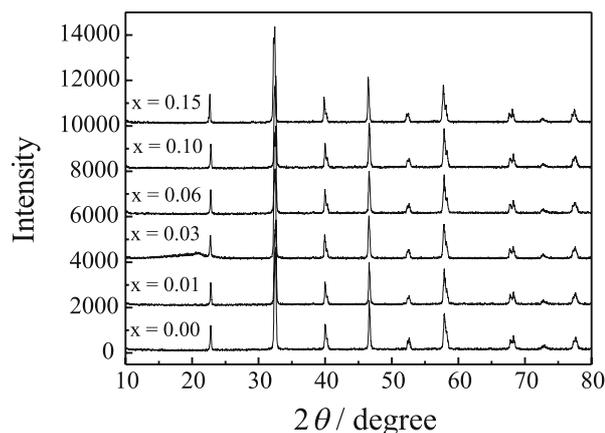
FIGURE 3   X-ray diffractograms of La$_{0.67}$Pb$_{0.33}$(Mn$_{1-x}$Fe$_x$)O$_{3+\delta}$ compounds sintered at 1000 °C in flowing oxygen. $x = 0.00, 0.01, 0.03, 0.06, 0.10$ and 0.15. Ni-filtered Cu K_α radiation

that phase pure material is obtained under these conditions (Fig. 2).

Figure 3 shows the XRD spectra of the La$_{0.67}$Pb$_{0.33}$ (Mn$_{1-x}$Fe$_x$)O$_3$ compounds sintered at 1000 °C in oxygen.

The crystal structure of the compounds was analysed in the rhombohedral space group ($R\bar{3}c$), hexagonal setting, using the X-ray powder diffraction data obtained at room

TABLE 2   Lattice parameters of the hexagonal and the rhombohedral unit cell of the La$_{0.67}$Pb$_{0.33}$(Mn$_{1-x}$Fe$_x$)O$_{3+\delta}$ samples sintered at 1000 °C

	Hexagonal unit cell			Rhombohedral unit cell		
x	a_h(Å)	c_h(Å)	V_h (Å^3)	a_r(Å)	α_r(deg.)	V_r(Å^3)
0.00	5.5218(1)	13.4101(3)	354.107(12)	5.4904(1)	60.3789(13)	118.036(4)
0.01	5.5243(1)	13.4109(3)	354.445(13)	5.4915(1)	60.3964(14)	118.148(5)
0.03	5.5258(1)	13.4123(4)	354.667(14)	5.4923(1)	60.4029(15)	118.222(5)
0.06	5.5281(1)	13.4105(3)	354.923(11)	5.4927(1)	60.4278(12)	118.308(5)
0.10	5.5282(1)	13.4108(3)	354.940(10)	5.4928(1)	60.4275(11)	118.313(4)
0.15	5.5257(1)	13.4112(2)	354.627(8)	5.4920(1)	60.4060(9)	118.209(3)
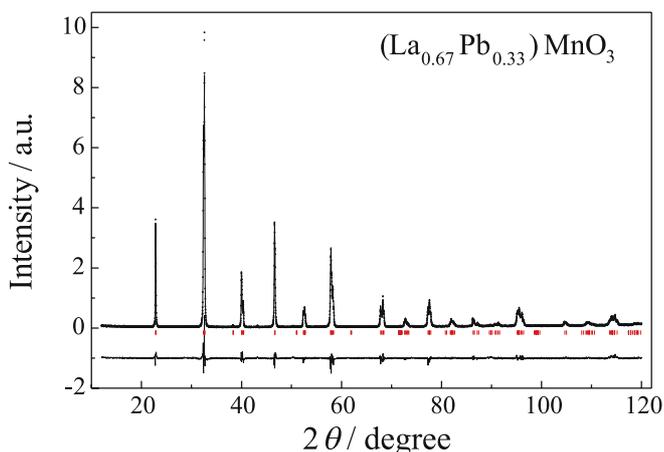
FIGURE 4   X-ray diffractogram with Rietveld refinement of (La$_{0.67}$Pb$_{0.33}$)MnO$_3$

FIGURE 6   Scanning electron micrograph of (La$_{0.67}$Pb$_{0.33}$)MnO$_{3+\delta}$ sintered in oxygen at 1000 °C

FIGURE 5   Energy dispersive X-ray fluorescence analysis of a crystallite of La$_{0.67}$Pb$_{0.33}$(Mn$_{0.85}$Fe$_{0.15}$)O$_3$
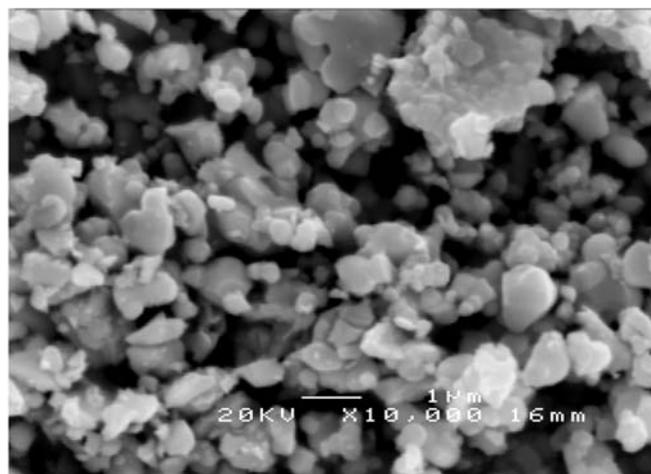
FIGURE 7   Scanning electron micrograph of (La$_{0.67}$Pb$_{0.33}$)(Mn$_{0.85}$Fe$_{0.15}$)O$_3$ sintered in oxygen at 1000 °C

temperature. The La atoms are at the (0, 0, 1/4) positions, Mn at (0, 0, 0) and O at (x, 0, 1/4). Figure 4 shows an example of the Rietveld refinement of the XRD pattern of (La$_{0.67}$Pb$_{0.33}$)MnO$_3$. The unit cell parameters obtained for these compounds after the Rietveld refinements are given in Table 2. These unit cell parameters are comparable to those reported in [6].

Energy dispersive electron fluorescence spectroscopy carried out on an individual crystallite of the La$_{0.67}$Pb$_{0.33}$(Mn$_{0.85}$Fe$_{0.15}$)O$_3$ clearly showed that Fe was incorporated into the manganate lattice. Although the Fe K_α line (6.404 keV) overlaps with the Mn K_β line (6.490 keV), the intensity of the line at 6.4 keV increased with increasing Fe contents and the Fe K_β line at 7.06 keV appeared (Fig. 5).

The oxygen stoichiometry of the samples sintered in air and in oxygen is given in Table 3. The value is close to three

although same samples, especially those sintered in oxygen were slightly overdoped.

Scanning electron microscopy of (La$_{0.67}$Pb$_{0.33}$)MnO$_{3+\delta}$ showed almost round-shaped crystallites with dimensions of 1 μm or less and some larger sintered agglomerates (Fig. 6). The (La$_{0.67}$Pb$_{0.33}$)(Mn$_{0.85}$Fe$_{0.15}$)O$_3$ sample had a similar microstructure, but the crystallites were polygonal (Fig. 7). These pictures show that practically no grain growth occurred during the sintering step.

The specific resistance (resistivity) increased slightly with the iron content up to a stoichiometry of 0.06 and then rather strongly for a stoichiometry of 0.10 (Fig. 8). Samples with an iron stoichiometry of 0.15 had a very high resistance,
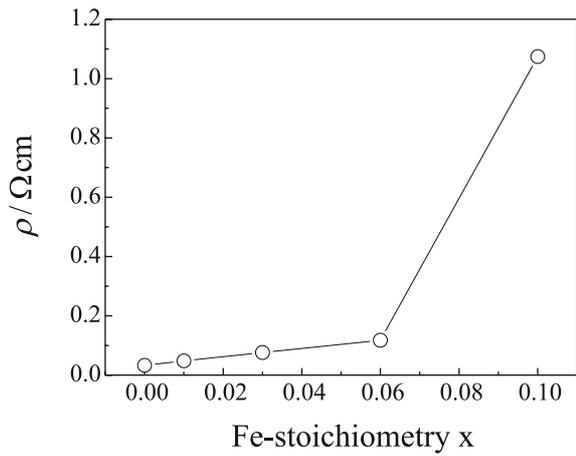
FIGURE 8   Specific resistance as a function of the Fe stoichiometry in La$_{0.67}$Pb$_{0.33}$(Mn$_{1-x}$Fe$_x$)O$_{3+\delta}$ compounds
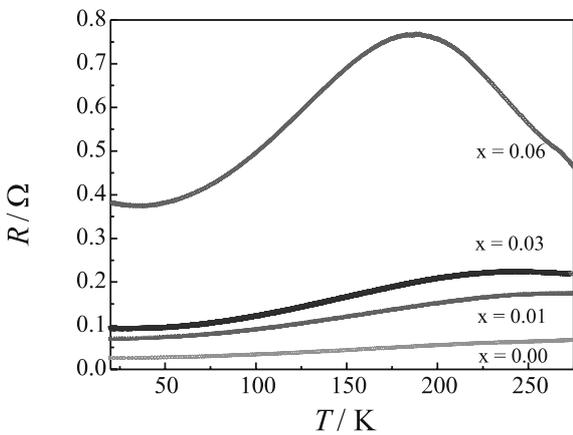
FIGURE 9   Temperature dependence of the resistance of La$_{0.67}$Pb$_{0.33}$ (Mn$_{1-x}$Fe$_x$)O$_{3+\delta}$ samples sintered at 1000 °C in oxygen
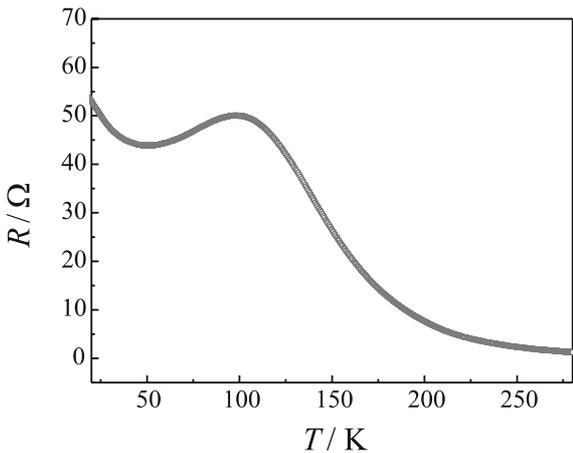
FIGURE 10   Temperature dependence of the resistance of a La$_{0.67}$Pb$_{0.33}$ (Mn$_{0.90}$Fe$_{0.10}$)O$_{2.99}$ sample

x	y (sintered in air)	δ	y (sintered in oxygen)	δ
0	3.03	+0.03	3.06	+0.06
0.01	3.01	+0.01	3.04	+0.04
0.03	2.98	−0.02	3.04	+0.04
0.06	3.02	+0.02	3.05	+0.05
0.1	3.03	+0.03	3.02	+0.02
0.15	3.02	+0.02	2.99	−0.01

TABLE 3   Oxygen stoichiometry of (La$_{0.67}$Pb$_{0.33}$)(Mn$_{1-x}$Fe$_x$)O$_y$ compounds sintered in air and in oxygen at 1000 °C
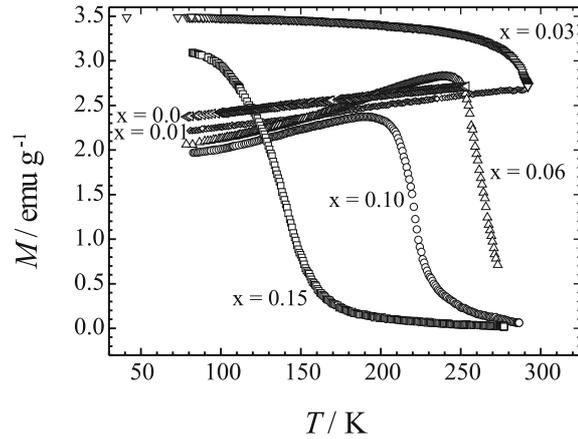
FIGURE 11   Magnetisation against temperature in magnetic field 50 Oe for La$_{0.67}$Pb$_{0.33}$(Mn$_{1-x}$Fe$_x$)O$_{3+\delta}$ samples. ($\triangleleft$) $x = 0.0$, ($\diamond$) $x = 0.01$, ($\triangledown$) $x = 0.03$, ($\triangle$) $x = 0.06$, ($\circ$) $x = 0.10$, ($\square$) $x = 0.15$
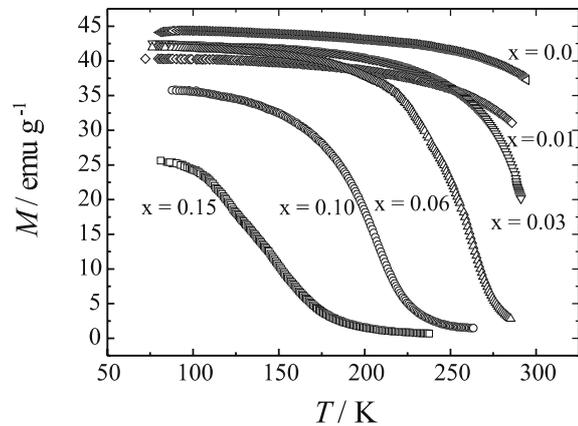
FIGURE 12   Magnetisation against temperature in a magnetic field of 1000 Oe for La$_{0.67}$Pb$_{0.33}$(Mn$_{1-x}$Fe$_x$)O$_{3+\delta}$ samples. ($\triangleleft$) $x = 0.0$, ($\diamond$) $x = 0.01$, ($\triangledown$) $x = 0.03$, ($\triangle$) $x = 0.06$, ($\circ$) $x = 0.10$, ($\square$) $x = 0.15$

which was difficult to measure. The temperature dependence of the resistance of the samples is given in Figs. 9 and 10. The sample with $x = 0.0$ shows metallic behaviour up to room temperature. Specimens with $x = 0.01$ and 0.03 indicate a change from metallic to insulating behaviour between 230 and 250 K. This change is quite pronounced for samples with $x = 0.06$ and occurs at 190 K. The compound with $x = 0.10$

exhibit insulating behaviour up to 50 K, metallic behaviour up to 100 K and then again insulating behaviour. This unusual temperature dependence of the resistance for samples with the composition La$_{0.67}$Pb$_{0.33}$(Mn$_{0..9}$Fe$_{0.1}$)O$_3$ agrees with published results [7].

The temperature dependence of the magnetisation at applied magnetic fields of 50 Oe and of 1000 Oe of the La$_{0.67}$Pb$_{0.33}$(Mn$_{1-x}$Fe$_x$)O$_3$ samples are shown in Figs. 11 and 12. The magnetisation data for the samples are comparable to those reported for samples with the composition $x = 0.0$, 0.05 and 0.1 [7]. The critical temperature T_C^M was defined as the inflection point of the $M(T)$ curve (i.e. the temperature corresponding to the minimum of dM/dT), at 50 Oe or at 1000 Oe. The following critical temperatures were ob-

tained: ~ 345 K, ~ 320 K, ~ 295 K, 260 K, 215 K and 140 K for $x = 0$, 0.01, 0.03, 0.06, 0.10 and 0.15, respectively. The temperatures for $x = 0$, 0.01 and 0.03 were estimated from extrapolation of the experimental points to higher temperatures by a fifth order polynomial fit followed by differentiation of the curve. The error of these estimations is about 5 K. The T_C^M values show almost linear decrease with x. The Curie temperatures are different from the metal–insulator transition temperatures T_{M-I} defined as a maximum in the temperature dependence of the resistance. Polycrystalline compounds with small grain sizes often show rather big differences between T_C^M and T_{M-I} [9–11]. Such behaviour is caused by the spin-dependent scattering or tunnelling processes at the grain boundaries, by inhomogeneities, microcraks or macroscopic defects. This phenomenon is called "extrinsic" magnetoresistive effect as opposed to the "intrinsic" magnetoresistive effect observed in single crystals near or at T_C^M and viewed as canonical for double exchange (DE) interaction systems [12, 13]. In all studied compounds this "extrinsic" part of the resistance plays a predominant role.

The magnetic field dependences of magnetization at 77 K and at room temperatures of $La_{0.67}Pb_{0.33}(Mn_{1-x}Fe_x)O_3$ samples are shown in Figs. 13 and 14. The magnetic fields for saturation magnetization determined from Fig. 13 were found to be 2500 Oe at 77 K for all samples. This field is enough to reach saturation magnetization at room temperature for samples with a Fe content $x \leq 0.03$. For higher Fe contents the compounds remain unsaturated even in the highest magnetic field available by our magnetometer. The saturation magnetic moment continuously decreases with increasing amounts of iron. Our magnetisation results on $La_{0.67}Pb_{0.33}(Mn_{1-x}Fe_x)O_3$ reveal that substitution of iron suppresses double exchange interaction between manganese ions and strongly affects the magnetic, thermal and transport properties of the parent compound.

4   Summary

The magnetic transition temperatures T_C^M and saturation magnetic moments of the compounds studied showed an almost linear decrease with an increasing iron substitution x. The Fe-substitution of Mn-sites suppressed the double exchange interaction between the manganese ions and strongly affected the magnetic, thermal and transport properties of the parent compound.

In all studied compounds the "extrinsic" part of the resistance, which is related to the grain boundaries, plays a dominant role. This "extrinsic" part of the resistance is responsible for the broad maxima in the $R(T)$ curves observed below T_C^M in these compounds and defined as T_{M-I}.

FIGURE 13   Hysteresis loops of magnetization at 77 K of $La_{0.67}Pb_{0.33}$ $(Mn_{1-x}Fe_x)O_{3+\delta}$ samples. ($\triangleleft$) $x = 0.0$, ($\diamond$) $x = 0.01$, ($\triangledown$) $x = 0.03$, ($\triangle$) $x = 0.06$, ($\circ$) $x = 0.10$, ($\square$) $x = 0.15$
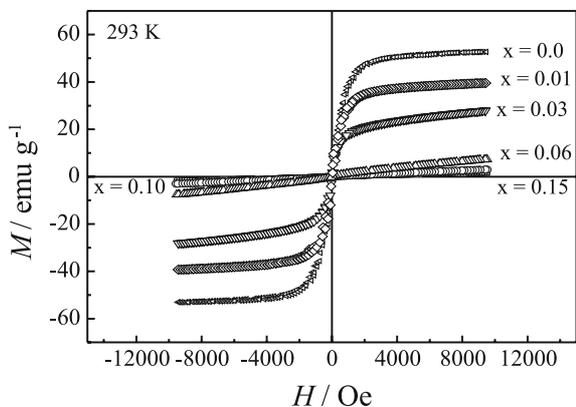
FIGURE 14   Hysteresis loops of magnetization at 293 K of $La_{0.67}Pb_{0.33}$ $(Mn_{1-x}Fe_x)O_{3+\delta}$ samples. ($\triangleleft$) $x = 0.0$, ($\diamond$) $x = 0.01$, ($\triangledown$) $x = 0.03$, ($\triangle$) $x = 0.06$, ($\circ$) $x = 0.10$, ($\square$) $x = 0.15$

REFERENCES

1   R. v. Helmolt, J. Wecker, B. Holzapfel, L. Schultz, K. Samwer: Phys. Rev. Lett. **71**, 2331 (1993)
2   C.N.R. Rao, B. Raveau: *Colossal Magnetoresistance, Charge Ordering and Related Properties of Manganganese Oxides* (World Scientific, Singapore 1998)
3   G.H. Jonker, J.H. van Santen: Physica **16**, 331 (1950)
4   A.H. Morrish., B.J. Evans, J.A. Eaton, L.K. Leung: Can. J. Phys. **47**, 2691 (1969)
5   M. Hoffmann, C. Niraimathi: Physica B **276**, 722 (2000)
6   J. Gutierrez, J.M. Barandiaran, A. Pena, L. Lezama, M. Insausti, T. Rojo, J. L Pizarro: J. Phys.: Condens. Matter **12**, 10523 (2000)
7   J. Gutierrez, A. Pena, J.M. Barandiaran, J.L. Pizarro, T. Hernandez, L. Lezama, M. Insausti, T. Rojo: Phys. Rev. B **61**, 9028 (2000)
8   Rodriguez-Carvajal: *'FULLPROF' Program, Rietveld Pattern Matching Analysis of Powder Patterns, ILL*, Grenoble 1990
9   R. Mahendiran, R. Mahesh, A.K. Raychaudhuri, C.N.R. Rao: Solid State Comm. **99**, 149 (1996)
10   R.D. Sánchez, J. Rivas, C. Vázquez-Vázquez, A. López-Quintela, M.T. Causa, M. Tovar, S. Oseroff: Appl. Phys. Lett. **68**, 134 (1996)
11   G.H. Rao, J.R. Sun, A. Kattwinkel, L. Haupt, K. Barner, E. Schmitt, E. Gmelin: Physica B **269**, 379 (1999)
12   B. Vertruyen, R. Cloots, A. Rulmont, G. Dhalenne, M. Ausloos, Ph. Vanderbemden: J. Appl. Phys. **90**, 5692 (2001)
13   J. Przewoźnik, J. Chmist, L. Kolwicz-Chodak, Z. Tarnawski, A. Kolodziejczyk, K. Krop, K. Kellner, G. Gritzner: Acta Phys. Polon. A **106**, 665 (2004)